Proceedings of the 2005 IEEE
International Conference on Robotics and Automation
Barcelona, Spain, April 2005

Parameters Selection and Stability Analysis of Invariant Visual Servoing with Weighted Features

N. García-Aracil, O. Reinoso
Universidad Miguel Hernández
Elche(Alicante), Spain
{*nicolas.garcia, o.reinoso*}*@umh.es*

E. Malis
I.N.R.I.A
Sophia Antipolis, France.
Ezio.Malis@sophia.inria.fr

R. Aracil
DISAM. UPM
Madrid, Spain
aracil@etsii.upm.es

***Abstract*— This paper concerns the continuity of vision-based robot control law. Recently, we have proposed a way of allowing the temporary disappearance of image features during the control task based on weighted features. Futhermore, we have redefined the camera invariant visual servoing approach in order to take into account the change of image features when zooming in or out during a positioning task. In this paper, we study ho to select some parameters of the weight function and we propose a local stability analysis of the invariant visual servoing approach with weighted features. Finally, experimental results demonstrate the improvements that can be achieved in the performance of vision-based control task.**

I. Introduction

The visibility problem in visual servoing tasks has received a particular attention in the last years [1], [8]. Research in this field has concentrated on visual servoing methods that are able to keep always the object in the field of view. In order to avoid that visual features leave the image, path planning in the image space is an elegant solution to the problem [8]. This approach allows to take into account several constraints like visibility, robot mechanical limits, etc . Contrary to the solutions that constraint the movements of the camera to assure the visibility of all features during the control task, we proposed in [2] the concept of allowing temporary disappearance of image features during the vision-based control task (Figure 1). The key idea of this approach consists in allowing some features to appear or disappear from the image (e.g features 1 and 4 go out of the image plane in sample T_K and then in sample T_{K+N} due to the movements of the camera they go back to the image plane) (Figure 1). The problem now is how to design a continuous control law when the information in the image change. This new approach has

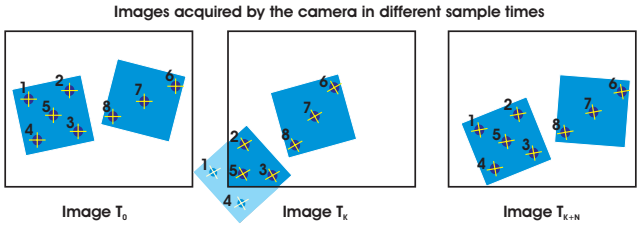

Fig. 1. The temporary disappearance of features in visual servoing control

been applied to the invariant visual servoing approach [5], [6]. Its reformulation was denominated invariant visual servoing approach with weighted features due to the use of a weight function to avoid the discontinuities produced by the changes of visibility in image features [2]. In this paper, we study how to select some the parameters of the weight function and we propose a local stability analysis. First of all, a short description of invariant visual servoing with weighted features is presented in Section II. The stability analysis of the invariant approach with weighted features is presented in Section III. The parameters selection of the weight function is presented and justified in Section IV. In the last section, some experimental results with an industrial robot are shown.

II. Theoretical Background

In this section, the theoretical fundamentals of invariant visual servoing with weighted features are presented. A more extensively description can be found in [2]. To take into account the changes of visibility in image features during the control task, a weight which depends on the position of the feature in the image plane is computed. The weights are used in order to anticipate in some way the possible discontinuities produced in the control law by the temporary disappearance of image features. Representing the weight as γ_y, the function that has been used and tested to compute the magnitude of the weights is:

$$\gamma_y(x) = \begin{cases} e^{-\frac{(x-x_{med})^{2n}}{(x-x_{min})^m(x_{max}-x)^m}} & x_{min} < x < x_{max} \\ 0 & x = \{x_{min}, x_{max}\} \end{cases} \quad (1)$$

The function weight $\gamma_y(x)$ is a bell-shaped function which is symmetrical respect to $x_{med} = \frac{x_{min}+x_{max}}{2}$.With n, m parameters, the shape of the bell function can be controlled. Their values must be chosen according to the following conditions:

$$\begin{cases} \gamma_y(x_{min} + \beta(x_{max} - x_{min})) & \geq 1-\alpha \\ \gamma_y(x_{min} + \frac{\beta}{2}(x_{max} - x_{min})) & \leq \alpha \end{cases} \quad (2)$$

where $0 < \alpha < 0.5$ and $0 < \beta < 0.5$. If the conditions (2) are verified then the following conditions are verified too:

$$\begin{cases} \gamma_y(x_{max} - \beta(x_{max} - x_{min})) & \geq 1-\alpha \\ \gamma_y(x_{max} - \frac{\beta}{2}(x_{max} - x_{min})) & \leq \alpha \end{cases} \quad (3)$$

where $0 < \alpha < 0.5$ and $0 < \beta < 0.5$. For each feature with (u_i, v_i) coordinates, a weight $\gamma_y(x)$ for its u_i and v_i

coordinates can be calculated using the definition of the function $\gamma_y(x)$ and has been denoted as ($\gamma_u^i = \gamma_y(u_i)$ and $\gamma_v^i = \gamma_y(v_i)$ respectively). In Figure 2(a), the representation of the $\gamma_y(x)$ function is shown. The two different zones and the shape that can be defined in the image plane can be seen in Figure 2.

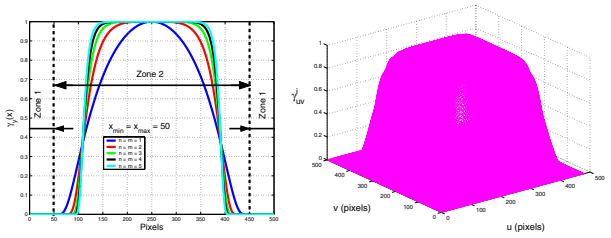

(a) $\gamma_u^i = \gamma_y(u_i)$ (b) $\gamma_{uv}^i = \gamma_u^i \cdot \gamma_v^i$

Fig. 2. Representation of the weight functions

The weights γ_{uv}^i mentioned above are *redistributed* in order to have $\sum \boldsymbol{\gamma_i}^2 = n$:

$$\boldsymbol{\gamma_i} = \sqrt{\frac{n}{\sum_{i=1}^{n} (\boldsymbol{\gamma_{uv}^i})^2}} \cdot \boldsymbol{\gamma_{uv}^i} \tag{4}$$

Suppose that n matched points are available in both images, current and reference. Every point has a weight γ_i which is used to build the following task function [10]:

$$\mathbf{e} = \mathbf{CW}\ (\mathbf{s} - \mathbf{s}^*(t)) \tag{5}$$

where $\mathbf{W}$ is a $(2n \times 2n)$ diagonal matrix where its elements are the weights γ_i. The derivative of the task function, considering $\mathbf{C}$ constant, is:

$$\dot{\mathbf{e}} = \mathbf{CW}\ (\dot{\mathbf{s}} - \dot{\mathbf{s}}^*) + \mathbf{C}\dot{\mathbf{W}}\ (\mathbf{s} - \mathbf{s}^*) \tag{6}$$

Substituting $\dot{\mathbf{s}} = \mathbf{L}\ \mathbf{v}$ in (6), we obtain:

$$\dot{\mathbf{e}} = \mathbf{CW}\ \mathbf{Lv} - \mathbf{CW}\dot{\mathbf{s}}^* + \mathbf{C}\dot{\mathbf{W}}\ (\mathbf{s} - \mathbf{s}^*) \tag{7}$$

A simple control law can be obtained by imposing the exponential convergence ($\dot{\mathbf{e}} = -\lambda \mathbf{e}$) of the task function to zero:

$$\begin{aligned} \mathbf{v} &= -\lambda\ (\mathbf{CWL})^{-1}\mathbf{e} + (\mathbf{CWL})^{-1}\mathbf{CW}\dot{\mathbf{s}}^* + \\ &+ (\mathbf{CWL})^{-1}\ \mathbf{C}\dot{\mathbf{W}}\ (\mathbf{s} - \mathbf{s}^*) \end{aligned} \tag{8}$$

where λ is a positive scalar factor which tunes the speed of convergence: Let us suppose that these weights γ_i are varying slowly, then $\dot{\mathbf{W}}$ can be considered nearly equal to zero ($\dot{\mathbf{W}} \approx 0$). Considering this assumption, the equation (8) can be rewritten as:

$$\mathbf{v} = -\lambda\ (\mathbf{CWL})^{-1}\mathbf{e} + (\mathbf{CWL})^{-1}\mathbf{CW}\dot{\mathbf{s}}^* \tag{9}$$

Setting $\mathbf{C} = (\mathbf{W}^*\mathbf{L}^*)^+$ (i.e. the matrices computed with the references values), if $(\mathbf{CWL}) > 0$ then the task function converges to zero and, in the absence of local minima and singularities, so does the error $\mathbf{s} - \mathbf{s}^*$.

Similarly to the standard invariant visual servoing [5], [7], the control of the camera is achieved by projecting the image features (current and reference) in the space $\mathcal{Q}^{\gamma_i}$. But in this case, $\mathcal{Q}^{\gamma_i}$ is variant respect the intrinsic parameters since it depends on the weights γ_i and they depend on the intrinsic parameters too. In order to be able to use this control approach with changes in intrinsic parameters during the control task, every sample time the weighted reference features $\mathbf{q}^*(t)$ must be computed with the weight γ_i calculated in function of the position of current feature in the image plane. Thus, the control of the camera is achieved by stacking all the reference points of space $\mathcal{Q}^{\gamma_i}$ in a $(3n \times 1)$ vector $\mathbf{s}^*(\boldsymbol{\xi}^*) = (\mathbf{q}_1^*(t), \mathbf{q}_2^*(t), \cdots, \mathbf{q}_n^*(t))$. Similarly, the points measured in the current camera frame are stacked in the $(3n \times 1)$ vector $\boldsymbol{s}(\boldsymbol{\xi}) = (\boldsymbol{q}_1(t), \boldsymbol{q}_2(t), \cdots, \boldsymbol{q}_n(t))$. If $\boldsymbol{s}(\boldsymbol{\xi}) = \boldsymbol{s}^*(\boldsymbol{\xi}^*)$ then $\boldsymbol{\xi} = \boldsymbol{\xi}^*$ and the camera is back to the reference position whatever the camera intrinsic parameters (Figure 3).

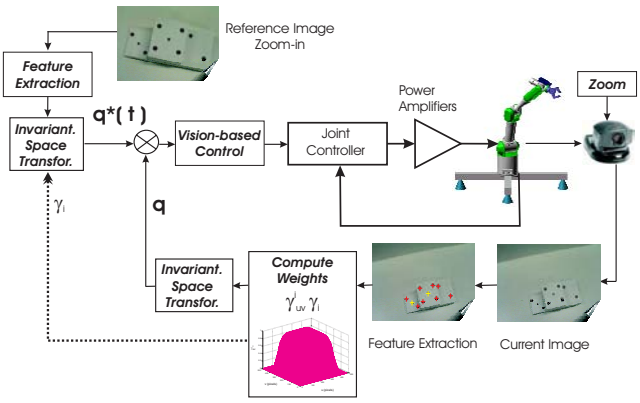

Fig. 3. Block diagram of the invariant visual servoing with weighted features.

In order to control the movement of the camera, we use the control law (9) where $\mathbf{W}$ depends on the weights previously defined and $\mathbf{L}$ is the interaction matrix. The interaction matrix in the weighted invariant space ($\boldsymbol{L}_{qi}^{\gamma_i} = \boldsymbol{T}_{mi}^{\gamma_i}\ (\boldsymbol{L}_{mi} - \boldsymbol{C}_i^{\gamma_i})$) is obtained like in [6] but the term $\boldsymbol{C}_{\boldsymbol{i}}^{\boldsymbol{\gamma_i}}$ must be recomputed in order to take into account the *r*edistributed weights γ_i.

III. Stability Analysis

In this section, the local stability of the control law is demonstrated. The local stability is valid only in a neighborhood of the equilibrium point. However, when the initial error is large, it is possible to sample the trajectory and consider only small errors at each iteration of the control law [7].

Considering the (6×1) task function mentioned before:

$$\boldsymbol{e} = (\boldsymbol{W}\ \widehat{\boldsymbol{L}})^+ \boldsymbol{W}(\boldsymbol{s} - \boldsymbol{s}^*(t)) \tag{10}$$

where $\mathbf{s}^*(\boldsymbol{\xi}^*) = (\mathbf{q}_1^*(t), \mathbf{q}_2^*(t), \cdots, \mathbf{q}_n^*(t))$, $\boldsymbol{s}(\boldsymbol{\xi}) = (\boldsymbol{q}_1(t), \boldsymbol{q}_2(t), \cdots, \boldsymbol{q}_n(t))$, $(\mathbf{W}\widehat{\mathbf{L}})^+$ is the pseudo-inverse of an approximation $\widehat{\mathbf{L}}$ of the true $(2n \times 6)$ interaction matrix and $\mathbf{W}$ is a $(2n \times 2n)$ diagonal matrix whose elements are the weights γ_i. We consider the most general case when $\widehat{\mathbf{L}}$

and $\mathbf{W}$ depends on $\mathbf{s}$. In that case :

$$\begin{aligned}\dot{\mathbf{e}} &= \frac{d(\mathbf{W}\widehat{\mathbf{L}})^{+}\mathbf{W}}{dt}(\mathbf{s}-\mathbf{s}^{*}) + (\mathbf{W}\widehat{\mathbf{L}})^{+}\mathbf{W}\ \dot{\mathbf{s}} - \\ &- (\mathbf{W}\widehat{\mathbf{L}})^{+}\mathbf{W}\ \dot{\mathbf{s}}^{*} \end{aligned} \quad (11)$$

Using the equation $\dot{\mathbf{s}} = \mathbf{L}\mathbf{v}$ and since the vector $\frac{d\ ((\mathbf{W}\mathbf{L})^{+}\mathbf{W})}{dt}(\mathbf{s}-\mathbf{s}^{*})$ can be written as $\frac{d\ ((\mathbf{W}\mathbf{L})^{+}\mathbf{W})}{dt}(\mathbf{s}-\mathbf{s}^{*}) = \mathbf{O}(\mathbf{s}-\mathbf{s}^{*})\mathbf{v}$ (where $\mathbf{O}(\mathbf{s}-\mathbf{s}^{*})$ is a 6×6 matrix such that $\mathbf{O}(\mathbf{s}-\mathbf{s}^{*})|_{\mathbf{s}=\mathbf{s}^{*}(t)} = 0$), we obtain:

$$\dot{\mathbf{e}} = (\mathbf{O}(\mathbf{s}-\mathbf{s}^{*}) + (\mathbf{W}\widehat{\mathbf{L}})^{+}\ \mathbf{W}\ \mathbf{L})\mathbf{v} - (\mathbf{W}\widehat{\mathbf{L}})^{+}\mathbf{W}\ \dot{\mathbf{s}}^{*} \quad (12)$$

Pluggin te equation $\mathbf{v} = -\lambda\mathbf{e} + (\mathbf{W}\widehat{\mathbf{L}})^{+}\mathbf{W}\dot{\mathbf{s}}^{*}$ in equation (12), the closed-loop equation is obtained:

$$\begin{aligned}\dot{\mathbf{e}} &= -\lambda[\mathbf{O}(\mathbf{s}-\mathbf{s}^{*}) + (\mathbf{W}\widehat{\mathbf{L}})^{+}\ \mathbf{W}\ \mathbf{L}]\mathbf{e} + \quad (13)\\ &+ \ [(\mathbf{O}(\mathbf{s}-\mathbf{s}^{*}) + (\mathbf{W}\widehat{\mathbf{L}})^{+}\ \mathbf{W}\ \mathbf{L} - \mathbf{I}\ ](\mathbf{W}\widehat{\mathbf{L}})^{+}\ \mathbf{W}\ \dot{\mathbf{s}}^{*}\end{aligned}$$

Applying the non-linear control theory to the system (14), we can say that it is locally asymptotically stable in a neighborhood of $\mathbf{s} = \mathbf{s}^{*}(t)$ (remember that $\mathbf{O}(\mathbf{s}-\mathbf{s}^{*})|_{\mathbf{s}=\mathbf{s}^{*}(t)} = 0$) if and only if the linearized system is stable:

$$\dot{\mathbf{e}} = -\lambda\mathbf{Q}\mathbf{e} + \mathbf{b}(t) \quad (14)$$

where :

$$\mathbf{Q} = (\mathbf{W}\widehat{\mathbf{L}})^{+}\ \mathbf{W}\ \mathbf{L}|_{\mathbf{s}=\mathbf{s}^{*}}$$

$$\mathbf{b}(t) = [(\mathbf{W}\widehat{\mathbf{L}})^{+}\ \mathbf{W}\ \mathbf{L} - \mathbf{I}\ ](\mathbf{W}\widehat{\mathbf{L}})^{+}\ \mathbf{W}\ \dot{\mathbf{s}}^{*}$$

Proposition 1: *In a neighborhood of* $\mathbf{s} = \mathbf{s}^{*}(t)$, $\mathbf{b}(t)$ *tends to zero when* $\mathbf{s}-\mathbf{s}^{*}(t) \to 0$

$\mathbf{b}(t)$ depends on $\dot{\mathbf{s}}^{*} = \frac{\partial\ \mathbf{q}^{*}(t)}{\partial\ t} \approx \frac{\mathbf{q}^{*}(t_{k+1})-\mathbf{q}^{*}(t_k)}{\Delta t}$. With γ_i, $\mathbf{p}_i^{*}$ and $\mathbf{p}_i^{\gamma_i *} = \gamma_i \cdot \mathbf{p}_i^{*}$, we can compute $\mathbf{q}^{*}(t_{k+1})$ and $\mathbf{q}^{*}(t_k)$:

$$\mathbf{q}_i(t_k) = \left(\mathbf{T}_{p^{*}}^{\gamma_i(t_k)}\right)^{-1}\mathbf{p}_i^{*}$$

$$\mathbf{q}_i(t_{k+1}) = \left(\mathbf{T}_{p^{*}}^{\gamma_i(t_k+1)}\right)^{-1}\mathbf{p}_i^{*}$$

where:

$$\begin{aligned}&\mathbf{q}_i^{*}(t_{k+1}) - \mathbf{q}_i^{*}(t_k) = \\ &= [\left(\mathbf{T}_{p^{*}}^{\gamma_i(t_k+1)}\right)^{-1} - \left(\mathbf{T}_{p^{*}}^{\gamma_i(t_k)}\right)^{-1}]\mathbf{p}_i^{*} \end{aligned} \quad (15)$$

$\mathbf{q}_i^{*}(t_{k+1}) - \mathbf{q}_i^{*}(t_k)$ only depends on the $\mathbf{T}_{p^{*}}^{\gamma_i}$. So if in equation (15), $\left(\mathbf{T}_{p^{*}}^{\gamma_i(t_k+1)}\right)^{-1} \approx \left(\mathbf{T}_{p^{*}}^{\gamma_i(t_k)}\right)^{-1}$ then $\mathbf{q}_i^{*}(t_{k+1}) - \mathbf{q}_i^{*}(t_k)$ is equal to zero and consequently $\mathbf{b}(t) = 0$.

Let us remember that $\mathbf{T}_{p^{*}}^{\gamma_i}$ computed for the same $\mathbf{p}^{*}$ reference features only depends on the variation of $\gamma_i(t)$. In a neighborhood of $\mathbf{s} = \mathbf{s}^{*}(t)$(when $\mathbf{s} \to \mathbf{s}^{*}(t)$), γ_i is nearly constant between two sample time because of its definition. So we have shown that $\left(\mathbf{T}_{p^{*}}^{\gamma_i(t_k+1)}\right)^{-1} \approx \left(\mathbf{T}_{p^{*}}^{\gamma_i(t_k)}\right)^{-1}$ then $\mathbf{b}(t) \to 0$ when $\mathbf{s} \to \mathbf{s}^{*}(t)$.

The linear system (14) is asymptotically stable *if and only if* $\mathbf{Q}$ has eigenvalues with positive real part and $\mathbf{b}(t)$ is bounded and tends to zero when $\mathbf{s}-\mathbf{s}^{*}(t) \to 0$:

$$\text{real}(\text{eig}(\mathbf{Q})) = \text{real}(\text{eig}((\mathbf{W}\widehat{\mathbf{L}})^{+}\ \mathbf{W}\ \mathbf{L})) > 0$$

The matrix $\mathbf{Q}$ depends on two set of unknown estimated parameters: $\mathbf{Q} = \mathbf{Q}(\widehat{\boldsymbol{K}}, \widehat{\boldsymbol{z}})$. Obviously if $\widehat{\boldsymbol{K}} = \mathbf{K}$ and $\mathbf{z} = \widehat{\boldsymbol{z}}$ then $\mathbf{Q} = \mathbf{I}$ and the equation (14) can be rewritten as: $\dot{\mathbf{e}} = -\lambda\mathbf{e}$ and the system is stable.

If $\mathbf{Q}$ is full rank then $\mathbf{e} = 0$ is the only equilibrium point of the system (i.e. if $\|\mathbf{e}\|$ decreases then it decreases towards $\mathbf{e} = 0$). It is well known from control theory that if $\mathbf{Q} > 0$ then the norm of the task function $\|\mathbf{e}\|$ decreases to zero and $\mathbf{b}(t) \to 0$ too as it was proven in Proposition 1.

As already mentioned, the local asymptotic stability of the system can be proved considering the system linearized around $\mathbf{e} = 0$ and $\mathbf{b}(t) \approx 0$ (i.e. $\boldsymbol{\xi} = \boldsymbol{\xi}^{*}$ and γ_i is nearly constant):

$$\dot{\mathbf{e}} = -\lambda\mathbf{Q}(\boldsymbol{\xi})|_{\mathbf{e}=0}\ \mathbf{e} = -\lambda\mathbf{Q}(\boldsymbol{\xi}^{*})\mathbf{e}$$

where $\mathbf{Q}(\boldsymbol{\xi}^{*}) = (\mathbf{W}\widehat{\mathbf{L}}(\boldsymbol{\xi}^{*}))^{+}\mathbf{W}\mathbf{L}(\boldsymbol{\xi}^{*})$. The system is locally stable if $\mathbf{Q}(\boldsymbol{\xi}^{*}) > 0$ since in that case $\mathbf{Q}(\boldsymbol{\xi}^{*})$ has eigenvalues with positive real part. However, to prove the local asymptotic convergence of $\mathbf{e}$ to zero, we need also to show that $\mathbf{s}-\mathbf{s}^{*}$ never belongs to $Ker((\mathbf{W}\widehat{\mathbf{L}})^{+}\mathbf{W})$.This means that it exists a neighborhood $\mathcal{U}$ of $\boldsymbol{\xi}^{*}$ such that $\mathbf{e} = (\boldsymbol{W}\ \widehat{\boldsymbol{L}}(\boldsymbol{\xi^{*}}))^{+}\boldsymbol{W}(\mathbf{s}-\mathbf{s}^{*}) \neq 0$, $\forall\boldsymbol{\xi} \in \mathcal{U}$ (i.e $\mathbf{e} = 0$ only if $\mathbf{s}(\boldsymbol{\xi}) = \mathbf{s}^{*}$). Let us suppose that $\mathbf{s}(\boldsymbol{\xi}) \neq \mathbf{s}^{*}$ and therefore $\boldsymbol{\xi} \neq \boldsymbol{\xi}^{*} = 0$. if we compute the Taylor development of $\mathbf{s}(\boldsymbol{\xi})$ (second order) in a neighborhood of $\boldsymbol{\xi}^{*} = 0$ and multiply both sides of it by $\mathbf{W}$, we will obtain the following equation:

$$\mathbf{W}(\mathbf{s}-\mathbf{s}^{*}) = \mathbf{L}(\boldsymbol{\xi}^{*})\mathbf{W}\ \boldsymbol{\xi} + O^{2}(\boldsymbol{\xi}) \quad (16)$$

Multiplying by $\boldsymbol{\xi}^{T}(\mathbf{W}\widehat{\mathbf{L}}(\boldsymbol{\xi}^{*}))^{+}$ both sides of equation (16) and knowing that $\boldsymbol{\xi}^{T}(\mathbf{W}\widehat{\mathbf{L}}(\boldsymbol{\xi}^{*}))^{+} \neq 0$ since $\boldsymbol{\xi} \neq 0$ and $\mathbf{W}\widehat{\mathbf{L}}(\boldsymbol{\xi}^{*})$ is full rank, the following equation is obtained:

$$\boldsymbol{\xi}^{T}(\mathbf{W}\widehat{\mathbf{L}}(\boldsymbol{\xi}^{*}))^{+}\mathbf{W}(\mathbf{s}-\mathbf{s}^{*}) = \boldsymbol{\xi}^{T}\mathbf{Q}\ \boldsymbol{\xi} + O^{3}(\boldsymbol{\xi}) \quad (17)$$

Remember that $\mathbf{Q} = (\mathbf{W}\widehat{\mathbf{L}})^{+}\ \mathbf{W}\ \mathbf{L}|_{\mathbf{s}=\mathbf{s}^{*}}$. if $\mathbf{Q} = (\mathbf{W}\widehat{\mathbf{L}})^{+}\ \mathbf{W}\ \mathbf{L})(\boldsymbol{\xi}^{*}) > 0$ then $\boldsymbol{\xi}^{T}\mathbf{Q}\boldsymbol{\xi} \geq 2\sigma\|\boldsymbol{\xi}\|^{2}$, where $\sigma > 0$ is the minimum singular value of the positive definite matrix $\mathbf{Q} + \mathbf{Q}^{T}$. As $\boldsymbol{\xi}^{T}(\mathbf{W}\widehat{\mathbf{L}}(\boldsymbol{\xi}^{*}))^{+}\mathbf{W}(\mathbf{s}-\mathbf{s}^{*}) = 0$ when $\mathbf{s} = \mathbf{s}^{*}$ then:

$$0 \geq 2\sigma\|\boldsymbol{\xi}\|^{2} + O^{3}(\boldsymbol{\xi})$$

that means:

$$\|\boldsymbol{\xi}\|^{2} \leq |O^{3}(\boldsymbol{\xi})|$$

which is impossible since, by definition of $O^{3}(\boldsymbol{\xi})$, it exists a neighborhood of $\boldsymbol{\xi}^{*}$ in which:

$$\|\boldsymbol{\xi}\|^{2} > |O^{3}(\boldsymbol{\xi})|$$

Therefore, $\boldsymbol{e} = (\boldsymbol{W}\ \widehat{\boldsymbol{L}})^{+}\boldsymbol{W}(\boldsymbol{s}-\boldsymbol{s^{*}}) \neq 0$ if $\mathbf{s} \neq \mathbf{s}^{*}$ in a neighborhood of $\boldsymbol{\xi}^{*}$ and the system is locally asymptotically stable.

IV. Parameters Selection

The weight function (1) has four parameters (x_{min}, x_{max}, n and m) which affect the performance of the invariant visual servoing with weighted features. With them, the image plane can be divided virtually in two zones (Zone 1 and Zone 2, Figure 4 (b)) and the shape of $\gamma_y(x)$ can be controlled (Figure 2 (a)). The Zone 1 is the part of the image where the weights γ_{uv}^i are equal to zero due to the definition of $\gamma_y(x)$. The width of the Zone 1 can be controlled by the parameters x_{min} and x_{max}. In Figure 4 (a), the representation of $\gamma_y(x)$ for different values of x_{min} and x_{max} with n, m constant is shown.

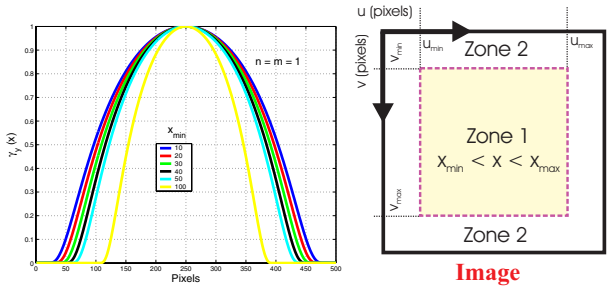

(a) Different widths of Zone 1 (b) Zone 1 and Zone 2

Fig. 4. Parameterization of Zone 1 and Zone 2

To show the effects produced by the values of n and m parameters of the weight function $\gamma_y(x)$ in the performance of the invariant visual servoing with weighted features, different experiments with simulated data have been carried out. One of them is the control of a camera that is moving from its reference pose due to a perturbation and at the same time is zooming in. The experiment has been repeat for different values of n and m (i.e. $n = m = i$ where $i = \{1,\ 2,\ 3,\ 4\}$). When n and m are increased, the shape of the function $\gamma_y(x)$ is more abrupt as it can be seen in Figure 2 (a). To show the performance of the system with the changes in n and m parameters, one component of the control law is shown in Figure 5. In this figure, the oscillations produced by the increment in n and m parameters can be seen. We want a control law to be as smooth as possible so the more suitable values for these parameters are 1.

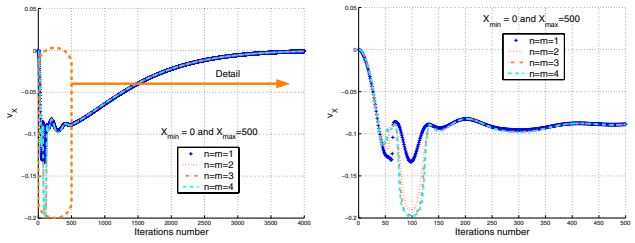

(a) v_X with different values of n and m (b) Detail of v_X

Fig. 5. Control law (v_X) with different values of n and m parameters

In the same way, the effects produced by the values of x_{min} and x_{max} parameters in the performance of the invariant visual servoing with weighted features can be seen in Figure 6. One component of the control law is shown in this figure and we can appreciate the increment in the number and magnitude of oscillations when the width of the Zone 2 is enlarged. In our control scheme, we are searching for a smooth control law to assure the best camera trajectory closer as much as possible to the optimal one.

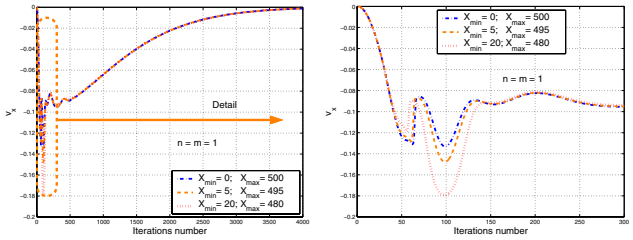

(a) v_X with different values of x_{min} and x_{max} (b) Detail of v_X

Fig. 6. Control law (v_X) with different values of x_{min} and x_{max} parameters

V. Experimental Results

Experimental results has been obtained using a 7 axis redundant Mitsubishi PA-10 manipulator (only 6 of its 7 d.o.f. have been considered). The experimental setup used in this work also include one camera (JAI CM 536) rigidly mounted at the robot end-effector, some experimental objects and two computers one of them with a Matrox Genesis vision board and the other with the PA-10 controller board (Figure 7). The goal of this experiment is keeping the robot in a reference position in spite of the fact that a perturbation is applied to the end-effector position of the robot. The amplitude and duration of this perturbation was chosen to produce that some image features go out of the image plane during the control.

We compare the weighted and un-weighted invariant visual servoing approaches. In this experiment, the interaction matrix is assumed constant and determined during off-line step using the desired value of the visual features and an approximation of the points depth at the reference camera pose. The goal of the control is to keep the robot in the reference position using the invariant visual servoing approach.

Using the invariant visual servoing approach, the system becomes unstable due to the lost of a feature during the control task(Figure 8). When the invariant visual servoing approach with weighted features is used, the system is stable although one or more features leave the image plane.

During the experiment, one feature go out of the image plane (feature with $(u_4,\ v_4)$ in Figure 8a). Due to the disappearance of this feature, a discontinuity is produced in the control law (Figure 8c-d). In Figure 8b, the robot end-effector velocities are shown. The system becomes unstable due to the lost of a feature during the control. In the second experiment, the new formulation of invariant visual servoing with weighted features was used. In this

experiment, the parameters of the weight function has been set to the suitable values described in Section IV.

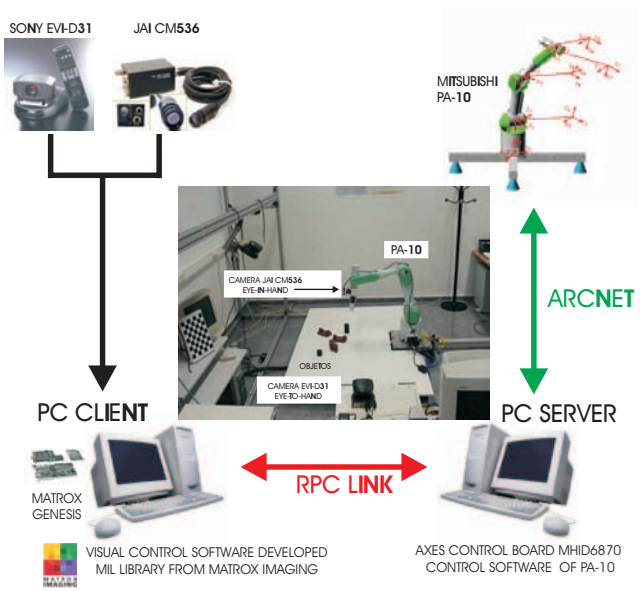

Fig. 7. Experimental Setup.

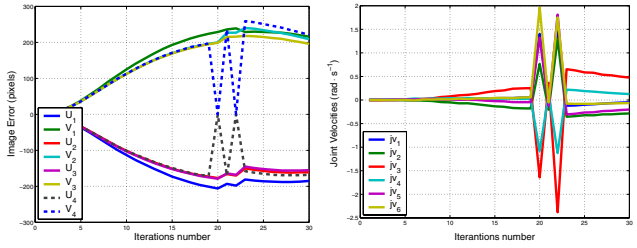

(a) Image error (b) Robot joints velocities

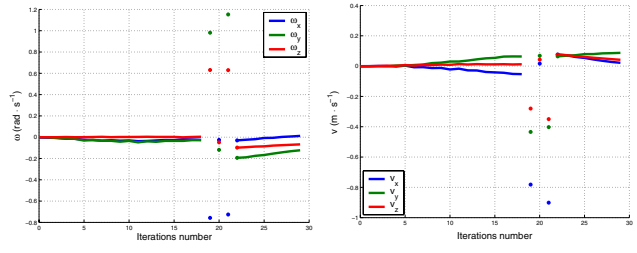

(c) Rotational velocity (d) Translational velocity

Fig. 8. Experimental results: invariant visual servoing approach

VI. Conclusion

In this paper, it has been shown that the invariant visual servoing with weighted features is locally stable in a neighborhood of the equilibrium point. To estimate accurately the size of this neighborhood is not easy since it depends on the uncertainties on the parameters of the system. Also the influence of the parameters of the weight function on the performance of the control law has been studied and a suitable selection of the values of them has been proposed and tested with a 6 d.o.f. eye-in-hand system composed by an industrial robot and a micro-head camera.

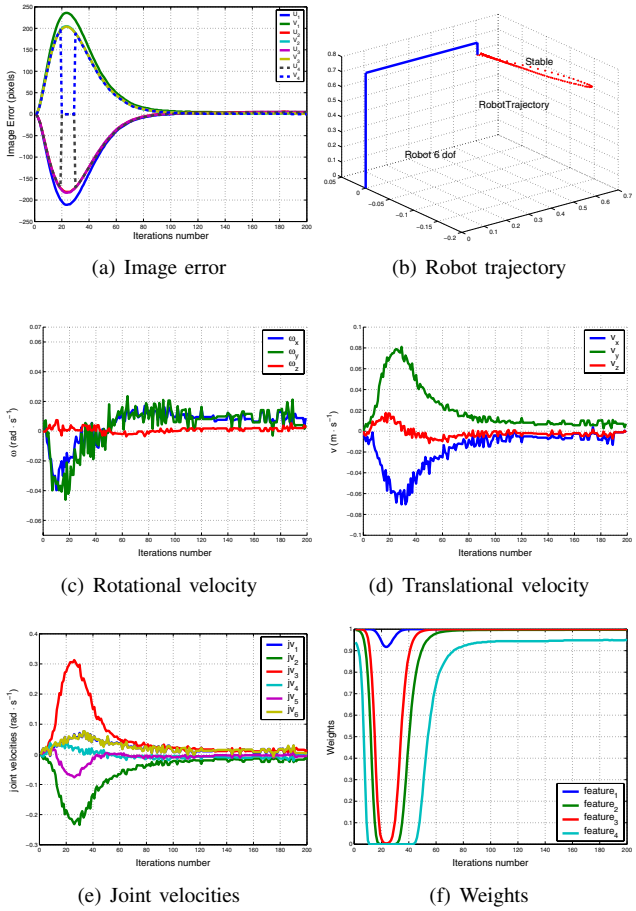

(a) Image error (b) Robot trajectory

(c) Rotational velocity (d) Translational velocity

(e) Joint velocities (f) Weights

Fig. 9. Experimental results: invariant visual servoing approach with weighted features.

References

[1] S. Benhimane and E. Malis Vision-based control with respect to planar and non-planar objects using a zooming camera In *IEEE International Conference on Advanced Robotics*, Coimbra, Portugal, July 2003.

[2] N. García and E. Malis. "Preserving the continuity of visual servoing despite changing image features" Proc. IEEE/RSJ International Conference on Intelligent Robots and Systems, Sendai, Japan, October 2004

[3] K. Hashimoto. *Visual Servoing: Real Time Control of Robot manipulators based on visual sensory feedback*, volume 7 of *World Scientific Series in Robotics and Automated Systems*. World Scientific Press, Singapore, 1993.

[4] S. Hutchinson, G. D. Hager, and P. I. Corke. A tutorial on visual servo control. *IEEE Trans. on Robotics and Automation*, 12(5):651–670, October 1996.

[5] E. Malis. Visual servoing invariant to changes in camera intrinsic parameters. In *International Conference on Computer Vision*, volume 1, pages 704–709, Vancouver, Canada, July 2001.

[6] E. Malis Stability Analysis of Invariant Visual Servoing and Robustness to Parametric Uncertainties. *Second Joint CSS/RAS International Workshop on Control Problems in Robotics and Automation*, Las Vegas, Nevada, December, 2002.

[7] E. Malis. Vision-based control invariant to camera intrinsic parameters: stability analysis and path tracking. In *IEEE International Conference on Robotics and Automation*, volume 1, Washington, D.C., USA, May 2002.

[8] Y. Mezouar, F. Chaumette Path Planning For Robust Image-based Control In *IEEE Trans. on Robotics and Automation*, 18(4):534-549, August 2002.

[9] Y. Mezouar, F. Chaumette Optimal Camera Trajectory with Image-Based Control *International Journal of Robotics Research*, 22(10-11):781-803, October-November 2003.

[10] C. Samson, M. Le Borgne, and B. Espiau. *Robot Control: the Task Function Approach*, volume 22 of *Oxford Engineering Science Series*. Clarendon Press, Oxford, UK, 1991.